PAPER

Design and validation of a microfluidic device for blood–brain barrier monitoring and transport studies

IOP Publishing Journal of Micromechanics and Microengineering
J. Micromech. Microeng. **28** (2018) 044001 (9pp) https://doi.org/10.1088/1361-6439/aaa816

Design and validation of a microfluidic device for blood–brain barrier monitoring and transport studies

Giovanni Stefano Ugolini[1,4], Paola Occhetta[1], Alessandra Saccani[2], Francesca Re[3], Silke Krol[2], Marco Rasponi[1,5] and Alberto Redaelli[1,5]

[1] Department of Electronics, Information and Bioengineering, Politecnico di Milano, Milan, Italy
[2] NanoMed lab, Fondazione IRCCS Istituto Neurologico Carlo Besta, Milan, Italy
[3] School of Medicine and Surgery, Nanomedicine center, NANOMIB University of Milano-Bicocca, Milan, Italy

E-mail: giovannistefano.ugolini@polimi.it

Received 25 July 2017, revised 5 December 2017
Accepted for publication 16 January 2018
Published 15 February 2018

Abstract

In vitro blood–brain barrier models are highly relevant for drug screening and drug development studies, due to the challenging task of understanding the transport mechanism of drug molecules through the blood–brain barrier towards the brain tissue. In this respect, microfluidics holds potential for providing microsystems that require low amounts of cells and reagent and can be potentially multiplexed for increasing the ease and throughput of the drug screening process. We here describe the design, development and validation of a microfluidic device for endothelial blood–brain barrier cell transport studies. The device comprises of two microstructured layers (top culture chamber and bottom collection chamber) sandwiching a porous membrane for the cell culture. Microstructured layers include two pairs of physical electrodes, embedded into the device layers by geometrically defined guiding channels with computationally optimized positions. These electrodes allow the use of commercial electrical measurement systems for monitoring trans-endothelial electrical resistance (TEER). We employed the designed device for performing preliminary assessment of endothelial barrier formation with murine brain endothelial cells (Br-bEnd5). Results demonstrate that cellular junctional complexes effectively form in the cultures (expression of VE-Cadherin and ZO-1) and that the TEER monitoring systems effectively detects an increase of resistance of the cultured cell layers indicative of tight junction formation. Finally, we validate the use of the described microsystem for drug transport studies demonstrating that Br-bEnd5 cells significantly hinder the transport of molecules (40 kDa and 4 kDa dextran) from the top culture chamber to the bottom collection chamber.

Keywords: trans-endothelial electrical resistance, drug development, blood brain barrier, microfluidics

Supplementary material for this article is available online

(Some figures may appear in colour only in the online journal)

1. Introduction

The blood brain barrier (BBB) is a functional biological structure of the central nervous system (CNS) that separates the vascular compartment of the brain from the cerebral

[4] Author to whom any correspondence should be addressed.
[5] These authors contributed equally to the work.

parenchyma. Peripheral blood vessels or capillaries normally exchange nutrients and small molecules with the surrounding tissue; however, in the CNS, endothelial cells forming the capillary walls exhibit tight junctions between each other yielding a highly controlled permeability to small molecules. This tighter endothelium does not exhibit fenestrations and the transport through the capillary walls is almost completely regulated by intra-cellular transport mechanisms. This peculiar function is referred to as BBB [1] and helps in preventing pathogens from reaching brain tissue. This barrier function, however, has the drawback of unselectively blocking the transport of hydrophilic molecules to the brain, which in turns also prevents pharmacological treatments of several CNS pathologies [2, 3].

Development of new drugs targeted to the CNS requires *in vitro* models to assess the potential of drug carriers or drug formulations to cross the BBB. Standard *in vitro* approaches involve the use of Transwell culture inserts where a tight endothelial monolayer is grown and transported molecules are collected in a lower chamber [4, 5]. The electric resistance of the cell monolayer (trans endothelial electric resistance, TEER) is the most common parameter to estimate barrier formation and is typically measured by means of chopstick-like pairs of electrodes manually inserted in the Transwell culture platform. This two-chamber model currently represents the standard culture system for BBB transport studies and has the advantage of being easily coupled to standard laboratory culture wells. The main disadvantages of this approach include the relatively high volumes required (hundreds of microliters to several milliliters depending on the insert size) and the manual handling of measurement electrodes leading to highly variable TEER results.

The fast rise of microfabrication technology enabled progress also in the field of *in vitro* BBB models. Indeed, the use of microfluidics has the advantage of reducing amounts of cells and reagents, holding particular potential in the development of drug screening microplatforms [6]. To date, a few examples of micron-scale culture systems for BBB studies are present in literature. The main microfluidic strategies to perform drug transport evaluation through the BBB are: trapping of cells into vertical micro-holes or posts to enable barrier formation and subsequent evaluation of molecules transported through the holes/posts in a collection channel [7–9]; tubular or 3D micro-structures resembling native blood vessels [10–12]; arrangements of porous membranes sandwiched between PDMS channels to perform standard 2D cell cultures and collect transported molecules in a lower collection chamber [13–17]. This last group of devices has been increasingly employed in recent research due to a higher similarity with standard 2D *in vitro* systems, an easier collection and detection of transported molecules and the possibility to monitor monolayer tightness by means of TEER measurements. However, technical limitations still affect this class of devices, since electrodes are usually integrated by complex sputtering procedures, or manually inserted on top of the culture chamber limiting optical visibility and being affected by positioning errors. In addition, higher channel resistances and different electric field distributions are known to be confounding parameters in scaling down the operations of commercial TEER monitoring systems [18].

We present a novel microfluidic device able to culture, monitor and study an endothelial barrier *in vitro*, representative of a BBB. We performed preliminary computational simulations to identify optimal electrodes position for performing TEER measurements; we employed standard soft-lithography to fabricate a multi-layer device featuring an upper culture chamber, a lower collection chamber and guiding channels for fine control of electrode position. Finally, we used this microfluidic device to culture murine brain endothelial cells. Investigations of tight junction formation, electrical resistance monitoring and transport studies demonstrated the effective formation of a brain endothelial barrier and the validity of the reported device for drug transport studies.

2. Materials and methods

2.1. Electrodes fabrication

Silver and platinum wires with a diameter of 250 μm were purchased from Sigma (Sigma-Aldrich, Milan, Italy). Current carrying electrodes—namely Pt electrodes—were fabricated by manually cutting platinum wire into short rods of about 1 mm length. Voltage sensing electrode—namely Ag/AgCl electrodes—were fabricated by cutting silver rods of about 1 cm length and depositing a thin layer of silver-chloride by means of an electrodeposition technique. Briefly, silver wires were cleaned for 10 min in nitric acid (1 M), rinsed with water and immersed in a 1 M HCl bath. Silver wires were then connected to the positive end of a power source. A platinum counter-electrode of same diameter and length was also immersed in the same bath and connected to the negative end of the power source. A constant current density of 1 μA cm^{-2} was applied to the system for 5, 15 or 30 min to obtain a coating of AgCl on the silver wires. The thickness of the layer was measured by cutting electrode cross-sections and analysis of microscopic images taken by a stereomicroscope.

2.2. Microdevice design

The microdevice comprises a porous polycarbonate (PC) membrane sandwiched between two fluidic layers (top culture chamber and bottom collection chamber). We designed top and bottom layer geometries in order to obtain two orthogonal chambers in the final multi-layer device configuration. For both layers, chamber height was set to 150 μm, chamber length to 5 mm and chamber width to 800 μm. This allows a square transport region (defined as the overlap between top and bottom chamber) of 800 $\times$ 800 μm. Four guiding channels (channel height 270 μm, channel width 270 μm) were designed to host electrodes of 250 μm diameter. In particular, one current carrying electrode was positioned in the upper layer and another in the lower layer to apply direct current through the culture membrane; voltage-sensing electrodes were positioned analogously. Each layer therefore contained one voltage electrode and one current electrode. The height of the culture chamber (150 μm) was kept smaller than that of

electrode channels (270 μm); this choice guarantees the electrodes to abut on a well-defined confinement spot, while still allowing their contact with the culture medium to ensure conductivity. The influence of voltage sensing electrode position (with respect to the transport region) on resistance measurement was investigated via numerical simulations and an optimal positioning of voltage sensing electrodes was identified. Details of numerical simulation methodologies are presented as supplementary materials (stacks.iop.org/JMM/51/044001/mmedia).

2.3. Master molds fabrication

The optimized two layer geometries were drawn through CAD software (AutoCAD, AutoDesk Inc.) and printed at high-resolution (32000dpi) in order to be used as photomasks in the master mold fabrication steps. In order to fabricate devices with different heights, two masks were printed per each layer, one including features to be printed with a height of 150 μm and one including features with 270 μm height.

Master molds fabrication was performed through standard photo-lithography techniques: a layer of SU-8 pre-polymer (MicroChem, Italy) was spin-coated on a clean silicon wafer to obtain a height of 150 μm. After soft-baking, the first mask was aligned and the wafer was exposed to UV light. After hard-baking, another layer of SU-8 pre-polymer was spin-coated on top of the previous layer in order to reach a total height of 270 μm. After soft-baking, the second mask was carefully aligned with the previous layer and the wafer was exposed to UV light. After a final hard-baking step the wafer was developed leaving the designed features in relief.

2.4. Layers fabrication

Top and bottom layers of the microdevices were realized through PDMS replica molding on the corresponding molds. PDMS was mixed at a 10:1 polymer to curing agent ratio and poured on the silicon wafers used as molds. After curing for 2 h at 65 °C, layers were peeled off the molds and the upper layer was punched to create channel inlet and outlet wells. Specifically, an inlet/outlet well diameter of 4 mm was used for top layer channel and 0.5 mm for bottom layer channel. The upper layer was also punched in correspondence of all four electrodes channels in order to create connections with external instrumentation for TEER measurement. To this aim, wells with a diameter of 2 mm were created at a distance of about 1 cm from the culture chamber. Porous PC membranes with a pore size of 3 μm and 10 μm thickness were purchased from Sigma (Whatman Cyclopore, Sigma-Aldrich, Italy). In order to fit the microdevices chambers, the membranes were cut into small squares of about 5 mm^2.

2.5. Microdevice assembly

Final microdevices consisted of four functional components: an upper PDMS layer; a porous PC membrane; Pt and Ag/AgCl electrodes; a lower PDMS layer. The device assembly was performed via toluene-PDMS stamp-and-stick bonding. This bonding technique employs a thin PDMS film as glue to stamp and assemble the upper and lower microdevice layers. Toluene was employed as an organic solvent to dilute PDMS, thus obtaining very thin glue layers that did not alter the channels geometries during stamping [19]. Curing agent, base PDMS and toluene (Sigma-Aldrich, Milan, Italy) were mixed in different ratios (1:10:0, 1:10:5, 1:10:10, 1:10:15) and spin-coated onto a clean silicon wafer (1500 rpm for 30″) to obtain a thin glue layer. Thickness of the glue layer was measured by curing it at 65 °C for 2 h, plasma bonding 1 cm^3 PDMS pieces on it, cutting the complex off the wafer and measuring the thin glue layer under a stereomicroscope.

Device assembly was performed as follows: upper and lower PDMS layers were stamped with uncured glue for 30 s and then lifted off. At this stage, the electrodes were manually inserted into the electrode channels matching the connection wells. The PC membrane was gently pressed on the top stamped layer until completely adhered to the PDMS. The lower layer was then carefully aligned under a stereomicroscope and brought into contact with the upper layer and PC membrane complex. Assembled microdevices were incubated at room temperature overnight to allow glue curing and then baked at 120 °C for 2 h to allow complete evaporation of toluene. Electrodes were then connected to electrical wires by means of a conductive epoxy resin (RS Components, Italy) poured in the connection wells.

2.6. Cell culture and monitoring

Microdevices were sterilized in ethanol overnight and coated with human fibronectin prior to cell seeding (25 μg ml^{-1}, 30 min incubation at 37 °C). Br-Bend5 murine endothelial brain cells were used at a cell suspension density of 5×10^6 cells ml^{-1}. After pre-loading both upper and lower layers with 30 μl of warm culture medium (10% FBS in DMEM), 10 μl of cell suspension were manually injected in the upper channel to perform cell seeding. Cells were allowed to adhere to the membrane for 4 h before adding additional 100 μl of culture medium. Control conditions were kept as devices filled only by culture medium and without cells. Cells were cultured in static conditions (no application of flow rate) and culture medium was refreshed every 24 h. Resistance values were recorded every 24 h by connecting the four electrodes to an EVOM voltammeter (WPI Instruments, Germany) via a custom-made RJ-10 connector. The resistance values of blank microdevices were subtracted to the recorded resistance values and the result was normalized to the square membrane transport region area to obtain TEER values.

2.7. Immunofluorescence

LIVE/DEAD assays (ThermoFisher, Italy) were performed after 5 days of culture by incubating the devices for 10 min with calcein/ethidium solution provided in the kit. After 5 d

of culture, cells were fixed with 4% paraformaldehyde and immunofluorescence was performed to assess endothelial tight-junction markers expression. After blocking and permeabilization for 1 h with 0.2% Triton-X in 3% BSA in PBS, cells were probed with appropriate primary/secondary antibodies solutions against ZO-1 (mouse monoclonal) and VE-Cadherin (rabbit polyclonal) (ThermoFisher).

2.8. Dextran permeability assay

After 5 days of culture, the transport of fluorescent dextran through the monolayer was evaluated. Medium was aspirated from all four inlet/outlet wells of the device. FITC-labeled 40 kDa- and 4 kDa dextran (Sigma-Aldrich) were diluted to a concentration of 1 mg ml^{-1} in culture medium. 30 μl of FITC-Dextran solution were injected in the upper layer whereas 30 μl of culture medium alone were injected in the lower layer. Fluorescent images were taken 10 min and 60 min after injection under an epi-fluorescence microscope. Image analysis was subsequently performed on ImageJ software: values of fluorescence intensity were obtained from lower compartments, corrected for background and normalized to fluorescence intensity in the upper compartment.

3. Results

3.1. Electrodes fabrication

Ag/AgCl electrodes were fabricated by electrodeposition of AgCl on Ag wires. We optimized current exposure time in order to obtain uniform AgCl layers. We also measured AgCl layer thickness to estimate the final electrode size. Exposing Ag wires to prolonged (30 min) current negatively affected the AgCl coating uniformity with several regions undergoing AgCl detachment (figure 1(A)). This condition yielded AgCl layer thicknesses of about 15 μm (figure 1(B)). We found optimal conditions for the preparation of the AgCl electrodes by exposing Ag wires to electrodeposition for 15 min, thus obtaining more uniform AgCl layers of approximately 5 μm thickness. This thickness value leads to a total electrode diameter of 260 μm. This directed the design of the microdevice geometry in terms of electrode guiding channel width: we chose to design electrode channels that are 270 μm in width and height.

3.2. Microdevice design

Numerical simulations guided the positioning of voltage sensing electrodes by providing estimated voltage drops recorded at different voltage electrodes positions. We computed numerically the $\Delta\Delta V$ value, defined as the difference between voltage drops across upper and lower layer in blank (only culture medium) and barrier (with added cells resistance) conditions, for paired voltage electrode positions along the chambers side (figure 2(A)). The position of the current electrodes was kept fixed at the two chamber ends. We excluded from the calculation positions that would result in voltage electrodes positioned in the same side as current electrodes. We considered as optimal electrode positions the ones showing higher $\Delta\Delta V$ (better detection) while also being exposed uniformly to current density (better repeatability). Figure 2(A) shows the model geometry and electrode positions considered. Resulting $\Delta\Delta V$ values are plotted in table 1. The current density plot is shown in figure 2(B). The current is injected from position 1u and, on opposite chamber sides, the current density results to be uniform only between positions 46u-41u. We therefore selected as final electrode position surfaces number 46u-5b which exhibits higher $\Delta\Delta V$.

3.3. Microdevice fabrication

Figure 1(D) shows a final sketch of the microdevice geometry with top layer represented in blue, bottom layer in red and the porous polycarbonate membrane represented in green. Electrodes arrangement and electrode types are also highlighted in figure 1(D). The fabrication protocol was optimized in order to ensure functional and leakage-free microdevices, despite the embedding of thick electrodes and of a PC membrane between two microstructured PDMS layers. To this aim, we screened different parameters for obtaining the PDMS glue layer.

Employing uncured PDMS glue alone, without the addition of toluene, resulted in glue layers with high thicknesses (approx. 30 μm) that significantly altered or clogged microdevice channel geometries. Mixing toluene with uncured PDMS allowed to obtain thin layers (below 5 μm) of PDMS glue, even at lower toluene mixing ratios (1:10:5, figure 1(C)). However, the higher toluene mixing ratio (1:10:15), leading to glue thicknesses of approximately 3 μm, was selected as optimal as it resulted in a more uniform bonding of porous polycarbonate membranes. The overall device geometry and bonding procedure was compatible with the insertion of 250 μm-wide electrodes inside designed electrode channels and allowed efficient and leakage-free bonding of PDMS top and bottom layers with the porous membrane. A picture of a fabricated microdevice is shown in figure 1(E).

3.4. Electrical resistance monitoring

We cultured Br-Bend5 murine brain endothelial cells in the microdevices for 5 days and monitored the TEER daily by connecting a commercial voltammeter to the four probes of the fabricated microdevices. Figure 3(A) shows the representative TEER values obtained during a 5 days culture experiments. TEER values increased during culture time and peaked to about 200 $\Omega \times cm^2$ after 5 days of culture, suggesting the formation of an endothelial barrier. We report that the culture time required for TEER increase and the average TEER values are comparable to those published in literature and obtained with on-chip systems or in Transwell systems [14, 20]. No evidences of electrode damage or electrode cytotoxicity could be detected during the experiments: fluorescent LIVE/DEAD assays indeed demonstrated high cell viability after 5 days (figure 3(B)).

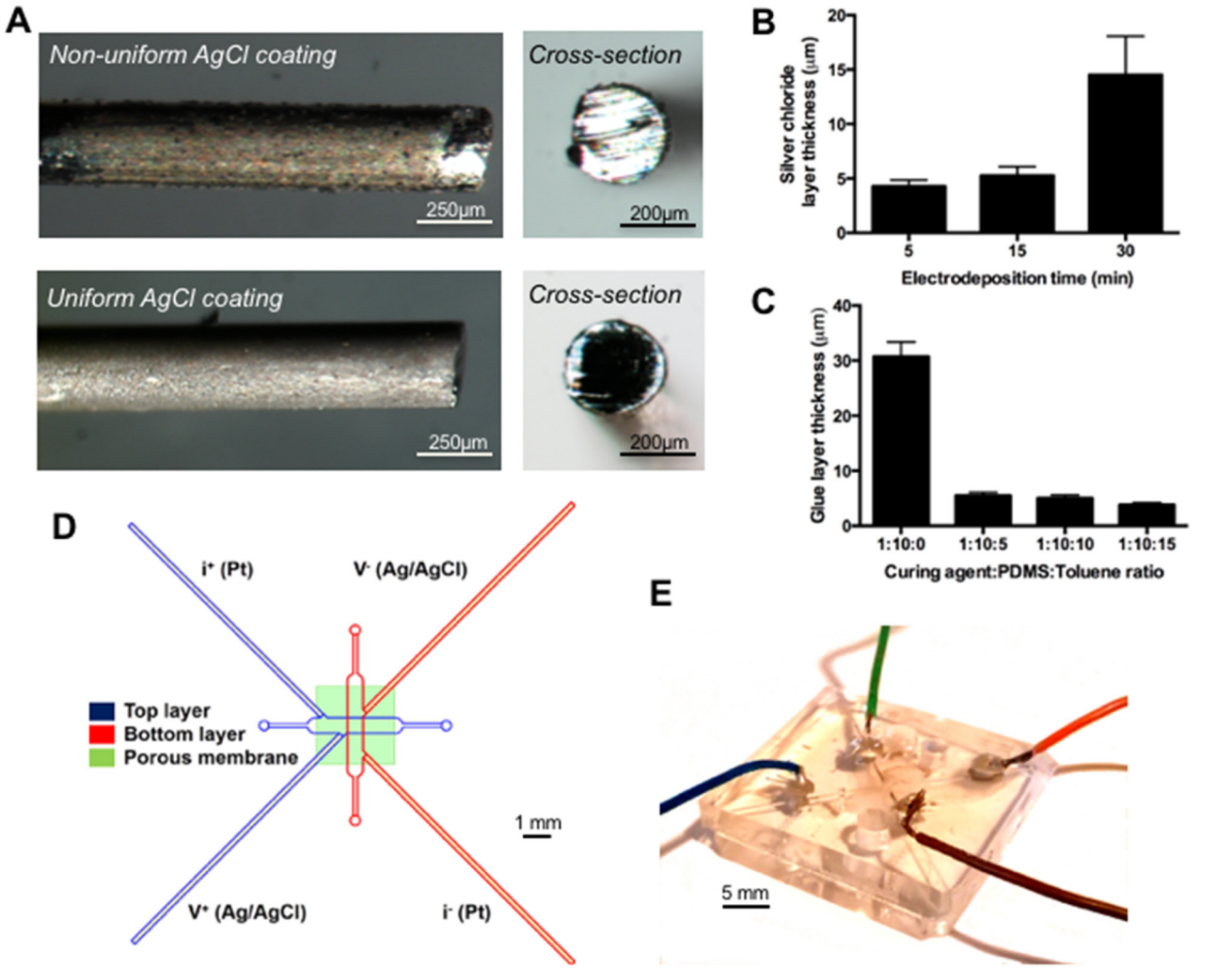

Figure 1. (A) Magnificated images of AgCl coated Ag wires (top views and cross-sections). Prolonged electrodeposition time causes thicker but non-uniform coatings (top) whereas shorter electrodeposition times lead to more uniformly coated electrodes. (B) Resulting AgCl coating thickness on Ag wires after 5, 15 or 30 min exposure to 1 μA cm^{-2} current density in a HCl bath. Prolonged exposure (30 min) to electrodeposition results in thick and non-uniform coatings of Ag wires (14.9 $\pm$ 4.5 μm) while shorter exposure times (15 min) result in thinner (5.1 $\pm$ 1.3 μm) and more uniform AgCl coatings. $n = 12$ measurements. (C) Resulting glue layer thickness after a fixed spin-coating rate and different toluene mixing ratio. Without addition of toluene glue layers results thick enough (30.3 $\pm$ 3 μm) to alter mirochannel structures. $n = 5$ tests (D) Sketch of the microdevice geometry: top PDMS layer is represented in blue, bottom PDMS layer in red while the porous polycarbonate membrane is represented in green. The electrode type (*V*, voltage electrode; *i*, current electrode) and electrode material (Ag/AgCl, silver chloride; Pt, platinum) are also highlighted. (E) Picture of a final microdevice featuring colored wires connected by epoxy conductive resin for connection to commercial voltohmeters.

3.5. Junctional markers

After 5 days culture period in the microdevices, we fixed cells and performed immunofluorescence in order to investigate the formation and localization of BBB tight junction markers. Cells were probed with antibodies against VE-Cadherin and ZO-1. VE-Cadherins regulate cell-cell adhesion and formation of junctions with reduced permeability, whereas ZO-1 has been more closely related to tight-junction formation in the BBB. Figures 3(C) and (D) show representative images of immunofluorescent staining obtained from cells cultured in microdevices. Cells show a specific membrane localization of ZO-1 and VE-Cadherin and a high degree of connections and coverage of the device. To further demonstrate uniformity of the tightly coupled endothelium, supplementary material S2 shows other fields of view of ZO-1 staining in the microdevices. This together with the increase in TEER demonstrates the ability of cells to form tight junctional complexes in monolayers cultured within the microdevices.

3.6. Permeability assays

After developing tight junctions and a uniform barrier (5 days culture time), we probed the endothelial monolayers in the microdevice with fluorescent dextran to assess the capability of hindering molecule transport. Figure 4(A) shows representative fluorescence images taken 10 min and 60 min after the injection of FITC-labeled 40 kDa and 4 kDa-Dextran

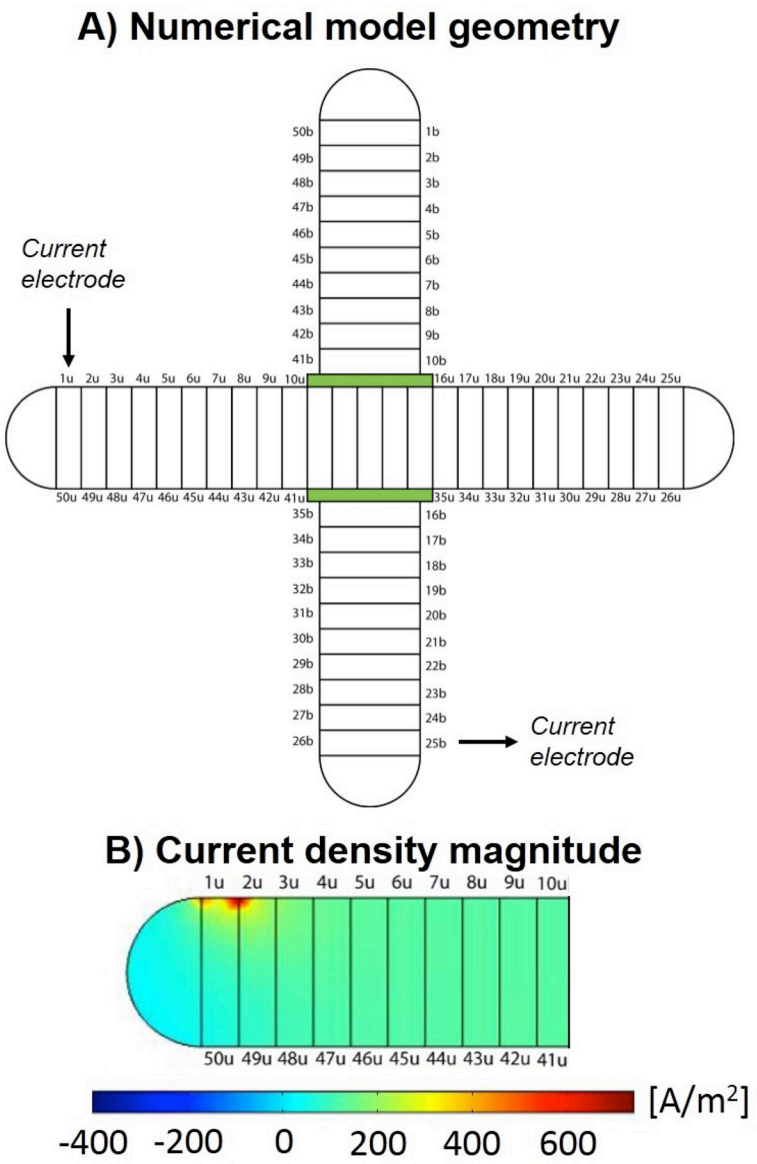

Figure 2. (A) Top view of the 3D numerical model employed for investigation of electrical parameters in the microdevice. The model comprises a top and bottom fluidic domains. The side surfaces are divided into 50 possible voltage electrode positions. A transport region domain is sandwiched between the two fluidic domains and is assigned culture medium parameters (blank condition) or cell resistance parameters (cultured microdevice condition). (B) 2D plot of current density norm inside a portion of the chamber. The current is injected from position 1u and, on opposite chamber sides, the current density results uniform only between positions 46u-41u.

into control devices and devices seeded with Br-Bend5 murine endothelial brain cells. Figure 4(B) also includes a quantification of fluorescence intensity in the two microfluidic compartments. Such analyses demonstrate that control devices allow free diffusion of dextran molecules into the lower chamber, as evidenced by the increase of fluorescence intensity in the bottom channel already after 10 minutes from injection and regardless of molecule size. On the other hand, significantly smaller values of fluorescence intensity of both molecules are detected in the bottom channels of devices seeded with Br-Bend5 cells up to 60 min from injection. This confirms the formation of an endothelial monolayer that hinders transport of both 40 kDa and 4 kDa dextran, thus highlighting a tighter barrier than non-brain endothelial cells (e.g. HUVECs [21, 22]).

4. Discussion

The optimization of robust BBB *in vitro* models is of significant importance to improve the development of drug formulations and drug carriers aimed at the central nervous system. In this respect, technical approaches based on microfluidic technologies are particularly promising due to the reduced platform sizes and the ability to incorporate measurement systems within the devices.

Indeed, the thriving field of microfluidic BBB models is characterized by a number of interesting reports detailing microfluidic devices capable of on-chip electrical monitoring of BBB endothelial monolayer formation and performing drug transport assays. Nevertheless, microdevices proposed in current literature are still hampered by complex fabrication

Table 1. Differences ($\Delta\Delta V$) between voltage drops across the membrane transport region in blank microdevice numerical models (only culture medium) and numerical models including the effect of cultured cells. The $\Delta\Delta V$ is computed for given current electrode positions and different voltage electrodes position in order to find maximum $\Delta\Delta V$ and improve the monitoring of TEER.

Voltage electrodes positions	$\Delta\Delta V$ (mV)	Voltage electrodes positions	$\Delta\Delta V$ (mV)	Voltage electrodes positions	$\Delta\Delta V$ (mV)
26u-50b	56,69	25u-1b	56,68	41u-10b	74,94
27u-49b	56,69	24u-2b	56,67	42u-9b	74,99
28u-48b	56,72	23u-3b	56,67	43u-8b	75,45
29u-47b	56,71	22u-4b	56,65	44u-7b	75,96
30u-46b	56,74	21u-5b	56,62	45u-6b	76,49
31u-45b	56,83	20u-6b	56,55	46u-5b	77,01
32u-44b	56,99	19u-7b	56,38	47u-4b	77,51
33u-43b	57,35	18u-8b	56,03	48u-3b	77,98
34u-42b	58,2	17u-9b	55,28	49u-2b	78,38
35u-41b	60,34	16u-10b	53,7	50u-1b	78,68

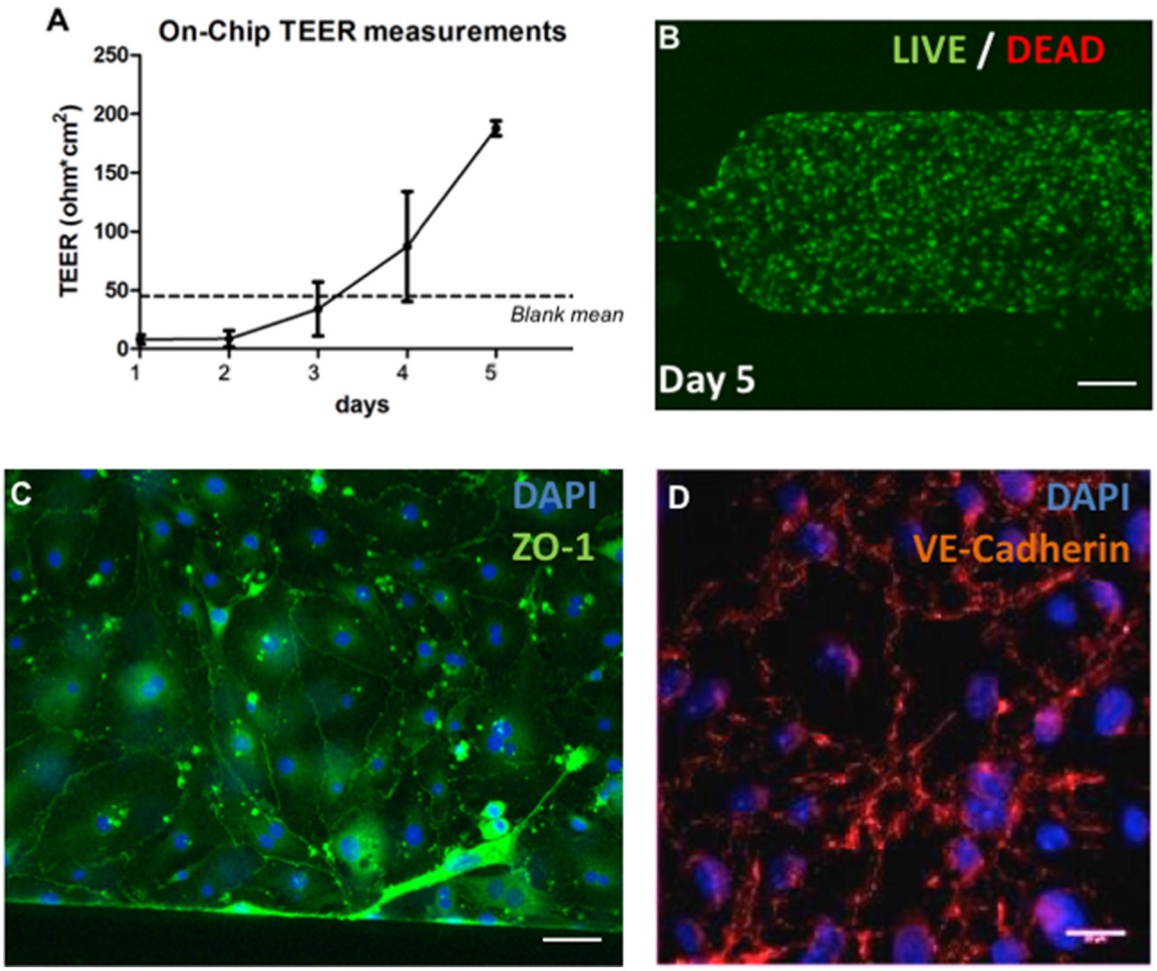

Figure 3. (A) TEER values recorded from cultured microdevices. TEER increases with culture time compared to blank devices, peaking at day 5 to a value of approximately 200 $\Omega \times \text{cm}^2$. $n = 4$ microdevices. (B) Representative image of a LIVE/DEAD fluorescent assay performed after 5 d of Br-Bend5 cell culture in the devices and demonstrating high cell viability. Scale bar = 200 μm. (C) Immunofluorescent images of murine Br-Bend5 cells fixed after 5 d culture time and stained for ZO-1 (tight junctions, green) and DAPI (nuclei, blue). Cells cover completely the culture chamber and exhibit membrane localization of ZO-1. Scale bar = 100 μm. (D) Immunofluorescent images of murine Br-Bend5 cells fixed after 5 d culture time and stained for VE-Cadherin (tight junctions, orange) and DAPI (nuclei, blue). Scale bar = 50 μm. Cells exhibit a membrane localization of VE-Cadherin, indicative of endothelial tight junctions formation.

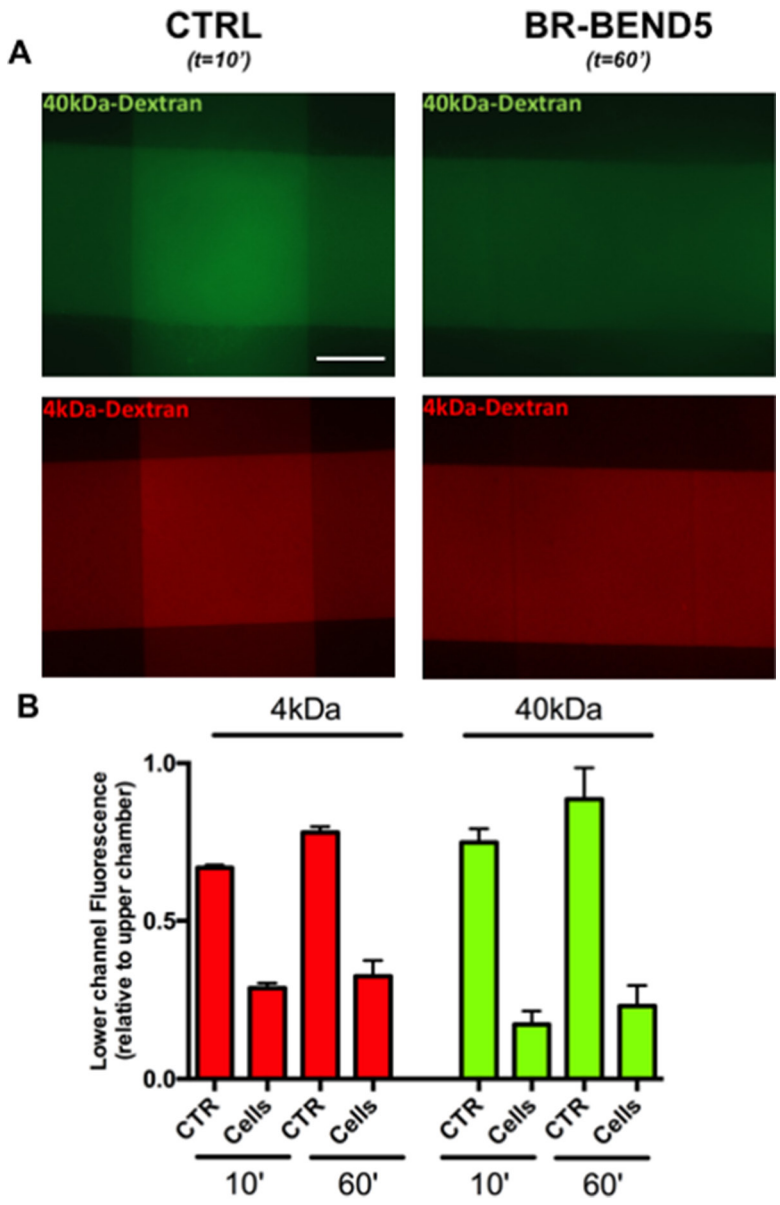

Figure 4. (A) Fluorescent images acquired from blank microdevices (left column) and microdevices cultured with Br-Bend5 for 5 d (right column). After the injection of FITC-labeled 40 kDa (green) and 4 kDa (red) dextran in the top culture chamber (placed horizontally in the images), images were taken after 10 min and 60 min from injection. (B) Fluorescence intensity quantifications in all experimental conditions. Values are expressed as fluorescence detected in the lower channel relative to fluorescence detected in the upper channels. Blank microdevices allow free diffusion of 40 kDa dextran as shown by the fluorescence intensity present in the bottom layer. In contrast, microdevices cultured with Br-Bend5 hinder 40 kDa and 4 kDa dextran transport.

protocols and assembly procedures. For instance, due to the inclusion of glass-based sputtered electrode layers, different reports present six-layers PDMS device [13, 15]. Other approaches include electrodes in simpler microdevice arrangements, but these lack control on their geometrical positioning and in some examples obstruct the optical visibility of the microdevices [23].

We here described the design, development and preliminary application of a multi-layer microdevice for *in vitro* modeling of the BBB. The device allows cell culture on a microporous membrane sandwiched between a top PDMS layer (for cell injection and culture) and a bottom PDMS layer (for collection of transported compounds). In addition to the possibility of performing transport studies, the device allows also for assessing TEER values by the included on-chip electrical monitoring system. This system comprises two pairs of electrodes for performing four-point resistance measurements. We employed numerical simulations to investigate optimal positioning of voltage sensing electrodes with respect to current electrodes. We opted for positioning voltage electrodes in order to meet uniform current density in the chamber while concurrently maximizing the voltage difference recorded between a blank device condition (culture medium) and a resistive device condition (cells resistance). The physical

electrodes are manually included into guiding channels during device fabrication. However, thanks to a design that provides electrode guiding channels slightly higher than the central chambers, the electrodes can precisely abut on the defined spots, thus improving reliability and repeatability of the fabrication procedure.

We performed in-depth biological validation of the presented BBB model, covering different aspects of endothelial barrier formation: analysis of TEER values, investigation of cellular junctional complexes formation and preliminary transport assays with a test compound. We showed that TEER increases with culture time, demonstrating functionality of the electrical measurement system. Accordingly, we showed how cells uniformly cover the culture chamber and form junctional complexes characterized by membrane localization of VE-Cadherins and ZO-1. Finally, we showed that the formed BBB is functional and hinders the transport of fluorescent 40KDa and 4kDa dextran. This globally validates the proposed platform for use in future translational studies involving transport of candidate drug formulations or nanosized drug carriers through the endothelial barrier.

5. Conclusions

We here presented a microdevice for culturing, electrical monitoring and chemical testing of brain endothelial monolayers. Thanks to a rigorous design approach, we optimized the electrical system design and fabrication in order to maintain simple device fabrication protocols while assuring repeatability of device features such as electrode positions. We showed that endothelial BBB monolayers cultured in the device exhibit tight functional junctions thus future applications of the device include drug screening validations.

Acknowledgments

This work was funded by Fondazione Cariplo, grant no. 2013-1048. This work was partially performed at Polifab, the micro- and nanofabrication facility of Politecnico di Milano.

Declarations

Competing interests: None declared
Ethical approval: Not required

ORCID iDs

Giovanni Stefano Ugolini https://orcid.org/0000-0003-4775-6676

References

[1] Weiss N, Miller F, Cazaubon S and Couraud P-O 2009 *Biochim. Biophys. Acta* **1788** 842
[2] Pardridge W M 2005 *NeuroRx* **2** 3
[3] Pardridge W M 2012 *J. Cereb. Blood Flow Metab.* **32** 1959
[4] Terasaki T, Ohtsuki S, Hori S, Takanaga H, Nakashima E and Hosoya K 2003 *Drug Discovery Today* **8** 944
[5] Wolff A, Antfolk M, Brodin B and Tenje M 2015 *J. Pharm. Sci.* **104** 2727–46
[6] Ugolini G, Cruz-Moreira D, Visone R, Redaelli A and Rasponi M 2016 *Micromachines* **7** 233
[7] Yeon J H, Na D, Choi K, Ryu S W, Choi C and Park J K 2012 *Biomed. Microdevices* **14** 1141
[8] Prabhakarpandian B, Shen M-C, Nichols J B, Mills I R, Sidoryk-Wegrzynowicz M, Aschner M and Pant K 2013 *Lab Chip* **13** 1093
[9] Deosarkar S P, Prabhakarpandian B, Wang B, Sheffield J B, Krynska B and Kiani M F 2015 *PLoS One* **10** e0142725
[10] Cho H, Seo J H, Wong K H K, Terasaki Y, Park J, Bong K, Arai K, Lo E H and Irimia D 2015 *Sci. Rep.* **5** 15222
[11] Alcendor D J *et al* 2013 *Stem. Cell Res. Ther.* **4** 1
[12] Adriani G, Ma D, Pavesi A and Kamm R D 2017 *Lab Chip* **17** 448–59
[13] Booth R and Kim H 2012 *Lab Chip* **12** 1784
[14] Kim Y *et al* 2014 *Proc. Natl Acad. Sci. USA* **111** 1078
[15] Wang Y I, Abaci H E and Shuler M L 2017 *Biotechnol. Bioeng.* **114** 184
[16] Brown J A *et al* 2015 *Biomicrofluidics* **9** 054124
[17] Ferrell N, Desai R R, Fleischman A J, Roy S, Humes H D and Fissell W H 2010 *Biotechnol. Bioeng.* **107** 707
[18] Douville N J, Tung Y C, Li R, Wang J D, El-Sayed M E H and Takayama S 2010 *Anal. Chem.* **82** 2505
[19] Chueh B H, Huh D, Kyrtsos C R, Houssin T, Futai N and Takayama S 2007 *Anal. Chem.* **79** 3504
[20] Yang T, Roder K E and Abbruscato T J 2007 *J. Pharm. Sci.* **96** 3196
[21] Ugolini G S, Visone R, Redaelli A, Moretti M and Rasponi M 2017 *Adv. Healthc. Mater.* **6** (https://doi.org/10.1002/adhm.201601170)
[22] Zervantonakis I K, Hughes-Alford S K, Charest J L, Condeelis J S, Gertler F B and Kamm R D 2012 *Proc. Natl Acad. Sci. USA* **109** 13515
[23] Griep L M, Wolbers F, De Wagenaar B, Ter Braak P M, Weksler B B, Romero I A, Couraud P O, Vermes I, Van Der Meer A D and Van Den Berg A 2013 *Biomed. Microdevices* **15** 145